Comparative Analysis of the Kinetic Characteristics of L-Type Calcium Channels in Cardiac Cells of Hibernators

Alexey E. Alekseev,*‡ Nick I. Markevich,* Antonina F. Korystova,* Andre Terzic,‡ and Yuri M. Kokoz*
Institute of Theoretical and Experimental Biophysics, Russian Academy of Sciences, Pushchino, Moscow Region, Russia; and ‡Division of Cardiovascular Diseases, Departments of Internal Medicine and Pharmacology, Mayo Clinic, Mayo Foundation, Rochester, Minnesota, USA

ABSTRACT An undefined property of L-type Ca^{2+} channels is believed to underlie the unique phenotype of hibernating hearts. Therefore, L-type Ca^{2+} channels in single cardiomyocytes isolated from hibernating versus awake ground-squirrels (*Citellus undulatus*) were compared using the perforated mode of the patch-clamp technique, and interpreted by way of a kinetic model of Ca^{2+} channel behavior based upon the concept of independence of the activation and inactivation processes. We find that, in hibernating ground-squirrels, the cardiac L-type Ca^{2+} current is lower in magnitude when compared to awake animals. Both in the awake or hibernating states, kinetics of L-type Ca^{2+} channels could be described by a $d^2f_1^2f_2$ model with an activation and two inactivation processes. The activation (or d) process relates to the movement of the gating charge. The slow (or f_1) inactivation is associated with movement of gating charge and is current-dependent. The rapid (or f_2) inactivation is a complex process which cannot be represented as a single-step conformational transition induced by the gating charge movement, and is regulated by β-adrenoceptor stimulation. When compared to awake animals, the kinetic properties of Ca^{2+} channels from hibernating ground-squirrels differed in the following parameters: (1) pronounced shift (15–20 mV) toward depolarization in the normalized conductance of both inactivation components, and moderate shift in the activation component; (2) 1.5–2-fold greater time constants; and (3) two-fold greater activation gating charge. Thus, L-type Ca^{2+} channels apparently switch their phenotype during the hibernating transition. Stimulation of β-adrenoceptors by isoproterenol, reversed the hibernating kinetic- (but not amplitude-) phenotype toward the awake type. Therefore, an aberrance in the β-adrenergic system can not fully explain the observed changes in the L-type Ca^{2+} current. This suggests that during hibernation additional mechanisms may reduce the single Ca^{2+} channel-conductance and/or keep a fraction of the cardiac L-type Ca^{2+} channel population in a non-active state.

INTRODUCTION

Hibernating animals, such as ground squirrels, hedgehogs or chipmunks, fall periodically into hibernation, which is characterized by a drop in body temperature from 37 to 5°C (Wang, 1978; Snapp and Heller, 1981). However, the drop in body temperature is a secondary phenomenon that follows changes in the primary integrative mechanism(s) of hibernating adaptation (Kondo, 1987; Heldmaier and Ruf, 1992; Kondo and Kondo, 1993). A prominent feature of the hibernating state is that the pronounced reduction in heart rate from 400 to less than 10 beats *per* min does not lead to death contrary to nonhibernating species (Lyman et al., 1982; Duker et al., 1983; Wang, 1978). Thus, hearts of hibernating species possess a unique cardioprotective phenotype with each hibernating cycle.

Whereas in nonhibernating species (e.g., guinea pig) cooling prolongs the plateau phase of the action potential, in hibernating animals (e.g., hedgehog) hypothermia shortens the plateau phase of the cardiac action potential (Duker et al., 1986; Burlington et al., 1989; Smith et al., 1989; Herve et al., 1992). This suggests that cardiac Ca^{2+} channels, which participate in the plateau phase of an action potential, have unique properties in hibernators. Indeed, in papillary muscles from hibernating chipmunks, Ca^{2+} current appears to be virtually absent, although in nonhibernating chipmunks this current does not differ from that of nonhibernating species (Kondo, 1986a). Because Ca^{2+} influx is essential for excitation-contraction coupling in cardiac muscle (Fabiato and Fabiato, 1979; Fabiato and Baumgarten, 1984), it has been postulated, on the basis of results obtained in multicellular preparations, that the initiation of myocardial contraction in hibernation may be triggered by Ca^{2+} influx through the Na/Ca exchanger or controlled through intracellular Ca^{2+} release mechanisms (Kondo and Shibata, 1984; Kondo, 1986b; Liu et al., 1991). However, in single cardiac cells during hibernation, we have demonstrated that Ca^{2+} current does flow through L-type Ca^{2+} channels, albeit dramatically reduced in magnitude, and could participate in the excitation-contraction coupling process during hibernation (Alekseev et al., 1994).

The dramatic reduction in inward Ca^{2+} current in hibernation may be due to several mechanisms including a decrease in the number of functional voltage-dependent Ca^{2+} channels (Kondo, 1986a), and/or a decrease in the cAMP-dependent phosphorylation of Ca^{2+} channels resulting from the decrease in the levels of circulating catecholamines (Gainullin and Saxon, 1988; Saxon and Gainullin, 1989). Yet, no definite characterization of the biophysical properties and regulation of voltage-dependent Ca^{2+} channels during hibernation has been performed. This is due in part

Received for publication 31 July 1995 and in final form 21 October 1995.
Address reprint requests to Dr. Alexey Alexeev, Division of Cardiovascular Diseases, Guggenheim 7F, Mayo Clinic, Rochester, MN 55905. Tel.: 507-284-4884; Fax: 507-284-9111; E-mail: aleka@mayo.edu.

0006-3495/96/02/786/12 $2.00

to the fact that studies have been conducted thus far almost exclusively in multicellular preparations or under hypothermic (but not under hibernating) conditions. Comparative analysis of the electrophysiological characteristics of Ca^{2+} channels during the hibernating versus the nonhibernating state are lacking. Herein, we analyzed the kinetic properties of L-type Ca^{2+} channels in cardiomyocytes isolated from ground squirrels during the hibernating and nonhibernating states, and establish the role of β-adrenoceptor-mediated regulation of L-type Ca^{2+} channels during hibernation.

MATERIALS AND METHODS

Isolation of single cardiac cells

Ground squirrels (*Citellus undulatus*) trapped at the end of summer in the Yakutia region of Siberia were kept under conditions close to natural. Experiments were performed on animals in two different physiological states: hibernation or spontaneous arousal (active). The body temperature of animals was 6–7.5°C during hibernation, and 37°C during spontaneous arousal. Single ventricular cardiocytes were isolated by the pronase/collagenase method described previously (see Alekseev et al., 1994).

Current recording

Currents were recorded by the perforated patch-clamp technique (Korn et al., 1991). Isolated cardiocytes were placed in a recording chamber and bathed with the following (in mM): 20 glucose, 5 $MgCl_2$, 2 $CaCl_2$, 10 HEPES, 80 NaCl, 20 tetraethylammonium chloride (TEA-Cl), 1.2 KH_2PO_4, and 10 CsCl (pH 7.3). Pipettes fabricated from soft molybdenum glass had a resistance of 1–5 MΩ and were filled with the following (in mM): 130 CsCl, 5 $MgCl_2$, and 10 HEPES (pH 7.3). The outward potassium current was blocked by TEA, and by replacing K^+ with Cs^+. Solutions were passed through a filter with a diameter of 0.22 mm (Millipore, Boston, MA). Amphotericin B (0.5 mg; Sigma Chemical Co., St. Louis, MO), which served as a perforating compound, was dissolved in 9 μl of dimethylsulfoxide and added to the pipette solution. The final concentration of the antibiotic was 200–250 μg/ml. Membrane permeabilization was completed within 10–15 min. Under these experimental conditions, recorded currents remained unchanged for 1.5–2 h. Experiments were carried out at room temperature (20–22°C). Currents, recorded with a patch-clamp amplifier ("Biopribor," Special Construction Bureau, Pushchino, Russia) integrated with a PCL-718 LabCard and an IBM AT/386 computer, were analyzed using the BioQuest software developed by A. E. A. and Y. M. K. Average values of the recorded parameters are presented as mean ± SE.

In cardiomyocytes from active ground squirrels, the three-dimensional current-voltage relationship, recorded as a response to a voltage-ramp at different holding potentials, possesses two distinct inward current components (see Fig. 1 *A*). The major component (peak 1) is sensitive to tetrodotoxin, reaches maximum at holding potentials more negative than −100 mV, and is related to the Na^+ current. The minor component (peak 2) is blocked by nifedipine, and is related to the Ca^{2+} current. Because at holding potentials between −60 and −70 mV only Ca^{2+} current could be recorded (see Fig. 1 *A*), measurements of Ca^{2+} current in cardiocytes from ground squirrels (both in hibernating and active states) were performed in this study without the use of a blocker of Na^+ channels.

Determination of kinetic parameters

Although kinetic parameters of various ionic currents in cardiocytes are usually determined from experimental records obtained by means of special stimulation protocols (Imaizumi et al., 1989; Langton et al., 1989), in the present study kinetic parameters were determined using one-pulse rectangular stimulation. To develop a kinetic model of Ca^{2+} current we used the modified Hodgkin-Huxley equations (Hodgkin and Huxley, 1952; Adams and Gage, 1979), and approximated experimental current curves by minimization (Himmelblau, 1972) using the Nelder-Meed method of deformed polyhedron. The parameters of the Ca^{2+} current model were determined using the least square method.

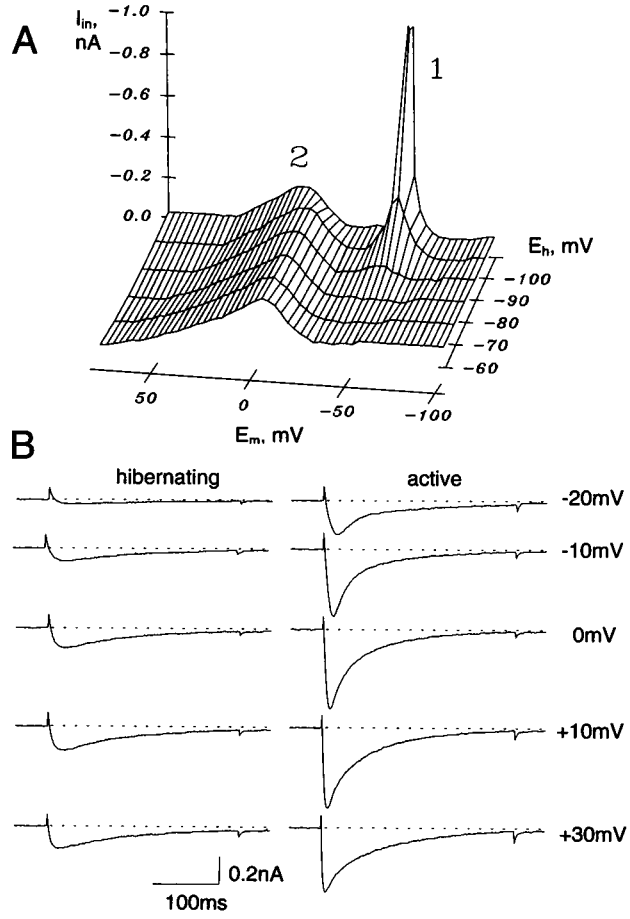

FIGURE 1 *A*: Three-dimensional reconstruction of the total inward current in isolated cardiocytes from active ground squirrel. Inward current (I_{in}, *z* axis) plotted as a function of membrane potential (E_m, *x* axis) and holding potential (E_h, *y* axis). Current-voltage relationships obtained for a voltage ramp of 1 V/s. *B*: Ca^{2+} currents of hibernating (*left*) and active (*right*) ground squirrels. Recordings made in response to depolarizing pulses to indicated membrane potentials (*right*). Holding potential, −60 mV. (· · · · ·) Zero current.

RESULTS

Existence of a reduced Ca^{2+} current in cardiomyocytes from hibernating ground squirrels

We compared voltage-dependent Ca^{2+} currents in cardiomyocytes isolated from ground squirrels during hibernation (Fig. 1 *B*, *left*) versus active state (Fig. 1 *B*, *right*) under the same experimental conditions. At each membrane potential (from −20 to +30 mV), the magnitude of the Ca^{2+} current was approximately threefold greater in active versus hibernating animals (Fig. 1 *B*). The average peak values of the Ca^{2+} current was −0.133 ± 0.02 nA (n = 26) and

-0.335 ± 0.04 nA ($n = 16$) in hibernating and in active ground squirrels, respectively. Thus, comparative analysis revealed that the Ca^{2+} current is reduced during hibernation (see also Alekseev et al., 1994).

Determination of kinetic parameters of Ca^{2+} current in hibernators: choice of model

The kinetic parameters of the voltage-dependent Ca^{2+} current in hibernators were determined by fitting the experimentally obtained Ca^{2+} current curves with the function derived from the modified Hodgkin-Huxley equation:

$$I_{Ca} = \overline{g_{Ca}} d^r f^s (E - E_{Ca})$$
$$\dot{d} = \frac{d_\infty - d}{\tau_d} \qquad (1)$$
$$\dot{f} = \frac{f_\infty - f}{\tau_f}$$

where I_{Ca} is the Ca^{2+} current, $\overline{g_{Ca}}$ is the maximal Ca^{2+} conductance, E_{Ca} is the equilibrium potential for the Ca^{2+} current; d_∞ and f_∞ are variables of Ca^{2+} channel activation and inactivation, and steady-state activation and inactivation parameters, which are functions of the membrane potential E; τ_d and τ_f are time constants of activation and inactivation, which are also functions of E; and r and s are the powers of the activation and inactivation variables.

To calculate the minimum χ^2, using the Nelder-Meed method, the parameters, d_∞ and f_∞, τ_d, τ_f, r, and s were chosen so that the solution to the system Eq. 1 describes most closely the experimentally obtained time course of the Ca^{2+} current (Fig. 2). The solution to the differential equations of system Eq. 1 was used as a function to calculate χ^2:

$$I = g_{Ca}(E - E_{Ca}) \cdot \{d_\infty - (d_0 - d_\infty)e^{-t/\tau_d}\}^r \cdot \{f_\infty - (f_0 - f_\infty)e^{-t/\tau_f}\}^s \qquad (2)$$

where d_0 and f_0 are the steady-state activation and inactivation current components at a given holding potential, respectively. Because the threshold of Ca^{2+} channel activation occurs at potentials more positive than the holding potential, we used the limiting values for these parameters ($d_0 = 0, f_0 = 1$).

According to the literature (e.g., Hagiwara and Nakajima, 1966), E_{Ca} in myocytes is of the order of 150 mV, and the value of g_{Ca} strongly depends on experimental conditions. Herein, g_{Ca} was determined from the slope of the right branch of the current-voltage curve for the peak current (Table 1; see also Fig. 3 *A*). Because experimentally obtained values of g_{Ca} were somewhat lower than the maximally achievable values because of the inactivation process, we used in most cases $E_{Ca} = 170$ mV, which is close to the upper theoretical limit. Actually, for values around 150–160 mV, we obtained kinetic parameters that did not essentially differ from the value obtained using 170 mV as the E_{Ca} value; however, with values <170 mV the fit of the experimental data with Eq. 2 (defined using the total mean-square error as the criterion) was not as adequate as with 170 mV.

The difference between the experimental and theoretical (obtained using Eq. 2) curves did not exceed a few percent (Fig. 2 *A*) regardless of the values for E and/or t, thus, indicating appropriate fitting. However, curves for $d_\infty(E)$ and $f_\infty(E)$ had a nonmonotonic shape even after varying the r and s parameters (i.e., (1, 2), (1, 4), and (2, 2)) (see Fig. 2, *B–D*) which makes difficult the interpretation of the activation and inactivation processes. Only by using $r = 2$, it was

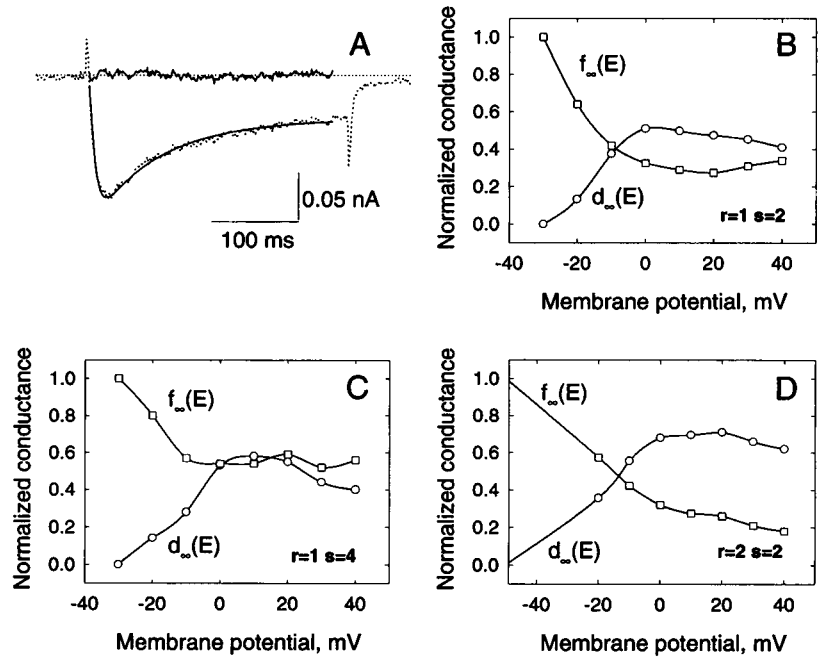

FIGURE 2 *A*: Experimental (*dotted*) and theoretical (*solid*) Ca^{2+} current curves. Theoretical curve obtained by fitting experimental data by Eq. 2. (·····) Zero current. Along the zero current line, the theoretical curve is subtracted from the experimental curve. *B–D*: Results of fitting currents at different values of r and s by Eq. 2. (○) Steady-state solutions for activation $d_\infty(E)$; (□) steady-state solutions for inactivation $f_\infty(E)$.

TABLE 1 Examples of kinetic parameters calculated by Eq. 4*

E, mV	I_{max}, nA	$d_\infty(E)$	τ_d, ms	$f_{1\infty}(E)$	τ_{f1}, ms	$f_{2\infty}(E)$	τ_{f2}, ms
−20	−0.120	0.395	5.57	0.538	96.2	0.875	0.78
−10	−0.268	0.641	6.54	0.325	76.9	0.825	31.2
0	−0.370	0.767	4.92	0.246	80.1	0.788	24.6
10	−0.393	0.790	3.64	0.174	120.2	0.686	16.9
20	−0.363	0.858	3.65	0.127	147.5	0.600	7.45
30	−0.312	0.938	3.46	0.108	159.1	0.462	4.76
40	−0.250	1.000	3.30	0.050	225.7	0.317	4.24
g_{Ca} = 5.76 nS		$E_d^{0.5}$ = −16.1 mV		$E_{f1}^{0.5}$ = −20.4 mV		$E_{f2}^{0.5}$ = 26.3 mV	
E_{Ca} = +170 mV		k_d = 16.4 mV		k_{f1} = −19.7 mV		k_{f2} = −21.3 mV	

*The results of fitting are exemplified in Fig. 4.

possible to approach a monotonous shape for the curve (Fig. 2 *D*). Thus, the kinetics of activation and inactivation of Ca^{2+} current measured in cardiocytes of hibernators cannot be represented as a monoexponential process within the frame of the model defined by the system Eq. 1. This agrees with the difficulty to describe the activation and inactivation of Ca^{2+} current as monoexponential processes (Imaizumi et al., 1989; Langton et al., 1989; Markwardt and Nilius, 1988).

To remain within the conventional interpretation of Ca^{2+} channel kinetics we modified the system Eq. 1, and involved two, instead of one, independent inactivation processes:

$$I_{Ca} = g_{Ca} d^r f_1^{s1} f_2^{s2} (E - E_{Ca})$$

$$\dot{d} = \frac{d_\infty - d}{\tau_d} \qquad (3)$$

$$\dot{f}_i = \frac{f_{i\infty} - f}{\tau_{fi}}, \quad i = 1, 2$$

where f_1 and f_2 are variables corresponding to the first and second inactivation process, respectively; τ_{f1} and

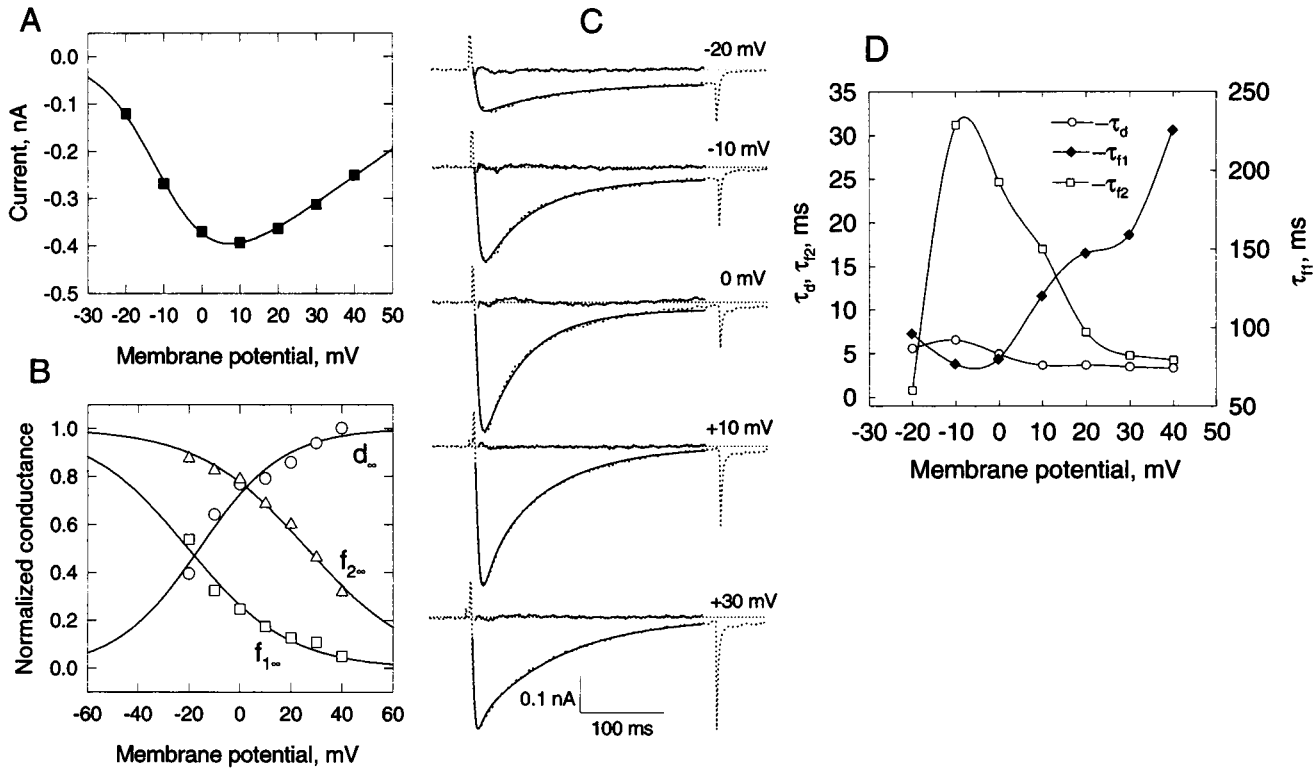

FIGURE 3 *A*: Current-voltage relationship constructed from the peak current values. g_{Ca}, calculated from the slope of right branch of the voltage-current relationship, is 5.76 nS. *B*: Normalized conductance versus membrane potential. (○) Activation; (□) slow inactivation; (△) rapid inactivation; (——) approximation by the Boltzmann equation (Eq. 5). *C*: Reconstruction of Ca^{2+} currents. (· · · ·, ——) Experimental and theoretical currents, respectively. Along the zero current line, the theoretical curve is subtracted from the experimental curve. *D*: Characteristic times of Ca^{2+} currents obtained by fitting the experimental data using Eq. 4.

τ_{f2}, the respective time constants; and s_1 and s_2, the respective exponents. The solution to the system Eq. 3 was used as a function to fit the experimentally obtained curves:

$$I = g_{Ca}(E - E_{Ca}) \cdot \{d_\infty - (d_0 - d_\infty)e^{-t/\tau_d}\}^r \cdot \prod_i \{f_{i\infty} - (f_{i0} - f_{i\infty})e^{-t/\tau_{fi}}\}^{s_i}, \quad i = 1, 2 \tag{4}$$

Using Eq. 4 to fit the experimentally obtained Ca^{2+} current curves, we calculated $d_\infty(E), f_{1\infty}(E), f_{2\infty}(E)$, τ_d, τ_{f1}, and τ_{f2}, for currents obtained in hibernating and active ground squirrels. The best fit of the experimentally obtained values to the model (defined by the criterion of the total mean-square error for all E and t values) was obtained at $r = 2$, $s_1 = 2$, and $s_2 = 1$.

Fig. 3 demonstrates that the use of Eq. 4 permits the expected dependence of all normalized conductance on the membrane potential (Fig. 3 *B*) and provides an insignificant discrepancy between the theoretical and experimental current curves (Fig. 3 *C*). Indeed, it can be seen that, through the entire range of membrane potentials, all dependencies that characterize steady-state activation and both inactivation processes possess the expected monotonic shape (Fig. 3 *B*). Consequently, these parameters can be well described by the Boltzmann equation:

$$\text{for activation} \quad d_\infty(E) = [1 + e^{(E_d^{0.5} - E)/k_d}]^{-1} \tag{5}$$

where E is the potential at which the steady-state activation reaches its half-value, and k_d is the slope parameter. Correspondingly for inactivation, $E_{f1}^{0.5}$, $E_{f2}^{0.5}$, k_{f1}, and k_{f2} denote the same parameters in the Boltzmann function. Table 1 shows typical kinetic parameters obtained using Eq. 4 and fitted by the Boltzmann equation (Eq. 5).

The present model of Ca^{2+} current (developed within the frame of the Hodgkin-Huxley theory) had to incorporate an additional parameter of the inactivation process to obtain a satisfactory description of the Ca^{2+} current kinetics in hibernators. As the additional inactivation component (f_2) had faster characteristic times when compared with the f_1-inactivation process (Fig. 3 and Table 1), we assigned f_2 to denote fast, and f_1 to denote slow inactivation throughout the text.

Kinetic scheme of Ca^{2+} current in hibernators

Based on the described model, the scheme of the kinetics of Ca^{2+} current in hibernators was defined. To this end, differential equations of system Eq. 3 were rewritten as:

$$\dot{d} = \alpha_d(1 - d) - \beta_d d$$
$$\dot{f} = \alpha_{fi}(1 - f_i) - \beta_{fi} f_i, \quad i = 1, 2;$$

where the rate constants α and β are related to the approximation parameters as follows:

$$\alpha_d = \frac{d_\infty}{\tau_d}, \quad \beta_d = \frac{1}{\tau_d} - \alpha_d;$$
$$\alpha_{fi} = \frac{f_{i\infty}}{\tau_{fi}}, \quad \beta_{fi} = \frac{1}{\tau_{fi}} - \alpha_{fi}, \quad i = 1, 2 \tag{6}$$

In terms of opening and closing of activation and inactivation gates, parameters α_d, α_{f1}, α_{f2} and β_d, β_{f1}, β_{f2} are rate constants for the opening and closing of the activation gate and the f_1- and f_2-types of inactivation gates.

Given that, depending on the value of r, s_1, and s_2, a channel has by convention two activation gates, two f_1 -type inactivation gates, and one f_2 -type inactivation gate, the scheme of activation and inactivation can be represented as:

$$\begin{array}{ccc} & d^{co} & \\ {\scriptstyle \alpha_d} \nearrow \swarrow {\scriptstyle \beta_d} & & {\scriptstyle \beta_d} \searrow \nwarrow {\scriptstyle \alpha_d} \\ d^{cc} & & d^{oo} \\ {\scriptstyle \beta_d} \searrow \nwarrow {\scriptstyle \alpha_d} & & {\scriptstyle \alpha_d} \nearrow \swarrow {\scriptstyle \beta_d} \\ & d^{oc} & \end{array} \tag{7}$$

where d^{cc} is the state of the channel in which two activation gates are closed, d^{co} and d^{oc} are states in which one gate is open whereas the other is closed, and d^{oo} is the state in which both gates are open. Considering that states d^{co} and d^{oc} are macroscopically indistinguishable:

$$D_2 \underset{\beta_d}{\overset{2\alpha_d}{\leftrightarrow}} D_1 \underset{2\beta_d}{\overset{\alpha_d}{\leftrightarrow}} D_0, \tag{8}$$

where $D_2 = d^{cc}$, $D_1 = (d^{co} + d^{oc})$, $D_0 = d^{oo}$.

Similarly, a kinetic scheme for slow inactivation (f_1-type inactivation) can be constructed. Here, f_1^{cc} denotes the state in which two gates are closed, f_1^{oc} and f_1^{co} denote the states in which one gate is closed whereas the other is open, and f_1^{oo} denotes the state in which both inactivation gates are open. Again, because states f_1^{oc} and f_1^{co} are indistinguishable, the kinetic scheme of slow inactivation can be transformed:

$$F_2 \underset{\beta_{f1}}{\overset{2\alpha_{f1}}{\leftrightarrow}} F_1 \underset{2\beta_{f1}}{\overset{\alpha_{f1}}{\leftrightarrow}} F_0, \tag{9}$$

where $F_2 = f_1^{cc}$, $F_1 = (f_1^{co} + f_1^{oc})$, $F_0 = f_1^{oo}$.

For the f_2-type inactivation:

$$G_1 \underset{\beta_{f2}}{\overset{\alpha_{f2}}{\leftrightarrow}} G_0, \tag{10}$$

where G_1 and G_o are the states with closed and open gates of the f_2-type, respectively. Thus, Eqs. 8, 9, and 10 compose a scheme of the Ca^{2+} current in hibernators.

Based on this scheme (Eqs. 8–10), we also constructed a more general kinetic scheme of the Ca^{2+} channel (not shown). This scheme involves 18 states of $D_iF_jG_k$ ($i, j = 0, 2$; $k = 0, 1$) with transitions between states occurring at rate constants defined in Eqs. 8–10 in accordance

with the principle of independence of activation and both inactivations.

To quantify the proposed model under baseline conditions, as well as after cAMP-dependent phosphorylation, Ca^{2+} currents in the absence and in the presence of a saturating concentration (Kurachi et al., 1989) of a β-adrenoceptor agonist, isoproterenol, were analyzed in ground squirrels, and the $d_\infty(E)$, $f_{1\infty}(E)$, $f_{2\infty}(E)$, τ_d, τ_{f1}, τ_{f2}, α_d, α_{f1}, α_{f2}, β_d, β_{f1}, and β_{f2} parameters calculated.

Kinetics of activation

The steady-state activation parameters (shown in Fig. 4 and Table 2) indicate that the normalized conductance of Ca^{2+} current (Fig. 4 *A*) in cardiomyocytes from hibernating and active ground squirrels are not markedly different, at least for potentials more positive than −10 mV.

Addition of isoproterenol (2 mM) shifted the activation curve by 10 mV toward hyperpolarization in myocytes from hibernating animals (Fig. 4 *A*). A significant difference between active and hibernating animals was observed in the rate constants of activation at all examined potentials (Fig. 4 *B*). This indicates that stimulation of β-adrenoreceptors modulates the kinetics of Ca^{2+} current activation. This finding is in accord with the hypothesis that insufficient phosphorylation of Ca^{2+} channels may occur in hibernating animals. However, if the lack of phosphorylation of Ca^{2+} channels during hibernation was the sole mechanism responsible for changes in Ca^{2+} current, then the magnitude of the shift induced by isoproterenol could be expected to be more pronounced.

TABLE 2 Averaged steady-state characteristics of Ca^{2+} current activation and effective valences of gating charge

	Active animals	Hibernating animals	Hibernating animals + isoproterenol
$E_d^{0.5}$, mV	−15.6 ± 4.7	−10.0 ± 2.0	−19.3 ± 3.0
k_d, mV	17.9 ± 1.5	14.6 ± 2.4	16.4 ± 1.3
α_d^0, ms^{-1}	0.195 ± 0.0182	0.110 ± 0.0146	0.204 ± 0.0480
β_d^0, ms^{-1}	0.088 ± 0.0136	0.049 ± 0.0073	0.060 ± 0.0144
z_d	1.52 ± 0.15	1.91 ± 0.22	1.60 ± 0.13

The relationship between constants α_d and β_d versus membrane potential (Fig. 4, *C* and *D*) for the activation kinetic scheme (see Eq. 8) shows that the slopes of the curves α_d and β_d are of an opposite sign (see also Fig. 5 *B*). This could indicate that the process of opening and closing of activation gates may be represented as a single stage conformational transition for Ca^{2+} channels in myocytes obtained during the hibernating and active states, and can be approximated as:

$$\alpha_d = \alpha_d^0 \cdot \exp\left(z_d \Theta \frac{FE}{RT}\right)$$

$$\beta_d = \beta_d^0 \cdot \exp\left(z_d(\Theta - 1)\frac{FE}{RT}\right)$$

This equation describes conformational transition related to the movement of gating charge z_d across the membrane.

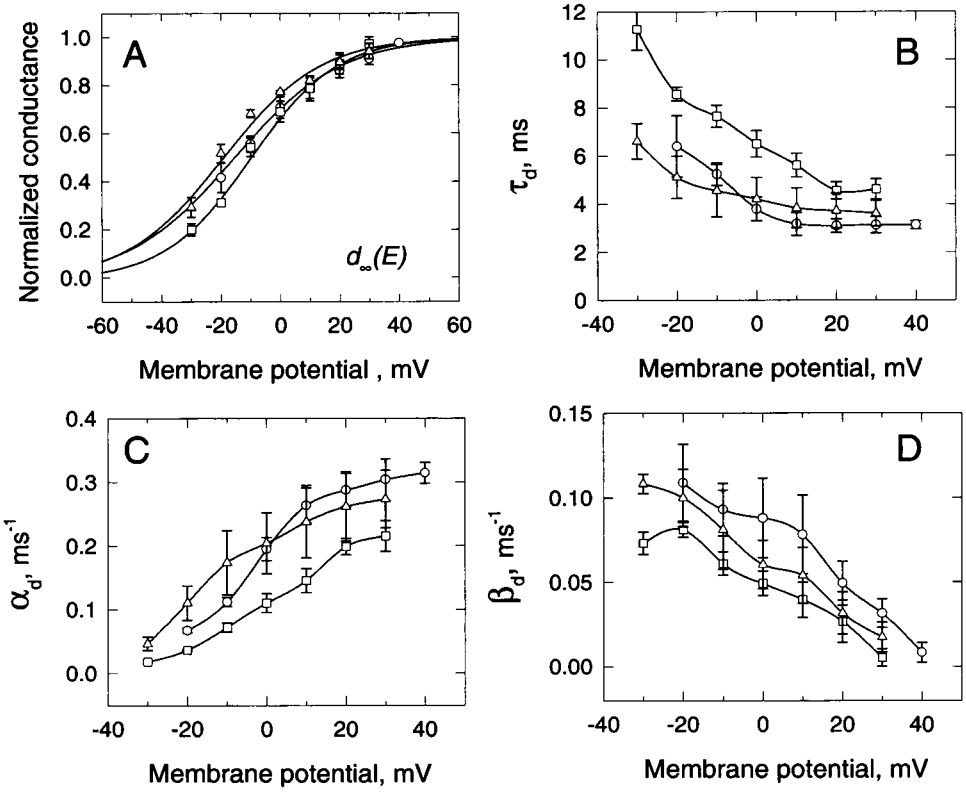

FIGURE 4 Averaged steady-state characteristics of Ca^{2+} current activation. (□) Hibernating; (○) active; (△) hibernating plus isoproterenol (n = 5). *A*: Normalized conductance. Solid curves are the result of fitting data by Eq. 5 (see also Table 2). *B*: Characteristic times of Ca^{2+} current activation. *C* and *D*: Rate constants for kinetic scheme (Eq. 8), as calculated from Eq. 6.

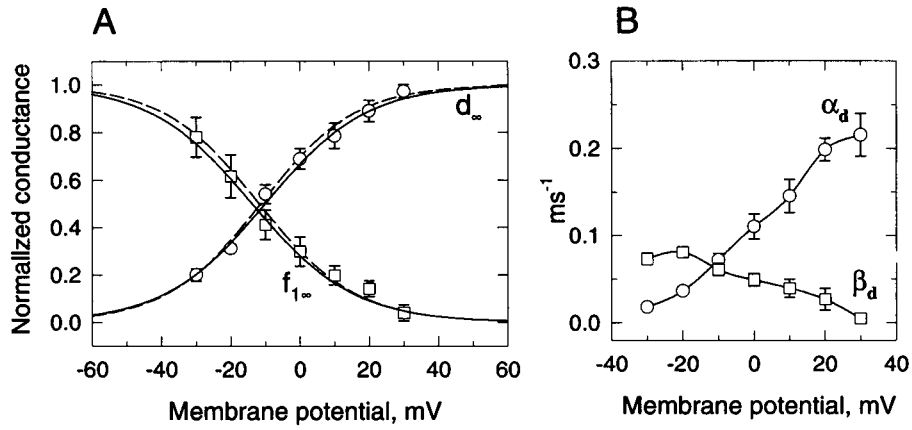

FIGURE 5 *A*: Normalized conductances calculated by approximating Ca^{2+} currents of hibernating ground squirrels using Eq. 4. Solid curves obtained by approximation of data using Eq. 5; dotted curves and obtained by calculation of gating charge z_d using Eq. 11. *B*: Averaged rate constants of kinetic scheme (Eq. 8) as calculated by fitting Ca^{2+} currents using Eq. 4.

Here α_d^0 and β_d^0 are the rate constants at $E = 0$ mV (Fig. 5 *B*); *F*, *R*, and *T* are the constants having a general meaning; Θ is the parameter characterizing the free energy of conformational transition, which lies between 0 and 1. The activation variable is approximated by the function:

$$d_\infty(E) = \left[1 + \frac{\beta_d^0}{\alpha_d^0} \exp\left(-z_d \frac{FE}{RT}\right)\right]^{-1}, \qquad (11)$$

from which the effective valence of activation gating charge z_d can be calculated. The results of fitting the averaged values (Fig. 5 *A*) using Eq. 11 are presented in Table 2.

Based on the scheme of Ca^{2+} channel activation (see Eq. 9), which suggests the presence of two activation gates, the total effective charge transferred by the gate subunits on activation of Ca^{2+} channels in active ground squirrels is estimated to be three elementary charges. This value is in good agreement with values reported for other species (Schneider and Chandler, 1973; Neely et al., 1993; Bangalore et al., 1995). Isoproterenol reversed the estimated number of elementary charges to the values calculated for myocytes from active squirrels (Table 2). Thus, at least in principle, a shift in the elementary charges, which appears to occur in hibernation, could be related to the lack of channel phosphorylation.

Kinetics of rapid inactivation

Fig. 6 presents averaged steady-state characteristics of rapid Ca^{2+} current inactivation in active and hibernating ground squirrels. Solid curves (Fig. 6 *A*) are constructed from the

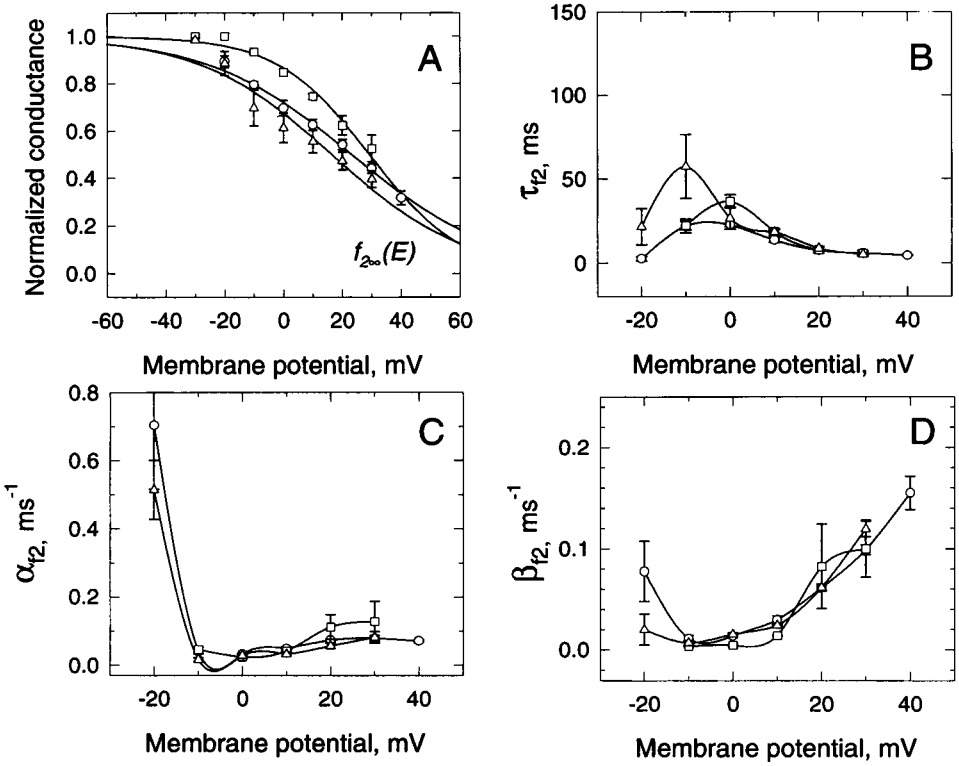

FIGURE 6 Averaged steady-state characteristics of fast Ca^{2+} current inactivation. *A*: Normalized conductance. Solid curves constructed using Eq. 5 (Table 3). *B*: Characteristic times. *C* and *D*: Constants of fast inactivation (kinetic scheme (Eq. 10)). [(squlo]) Hibernating; (○) active; (△) hibernating plus isoproterenol ($n = 5$).

results of approximation using the Boltzmann Eq. 5 (Table 3). A marked difference in the steepness of the inactivation curves between active and hibernating animals was obtained (Fig. 6 *A*).Therefore, in cardiocytes of hibernating ground squirrels, the contribution of the inactivation component to the total Ca^{2+} conductance at potentials more negative than 0–10 mV is negligible, whereas in cells of active animals it is significant (Fig. 6 *A*). Isoproterenol activates Ca^{2+} currents in cardiocytes of hibernating ground squirrels and shifts the normalized conductance of inactivation toward hyperpolarization and values characteristic for active animals (Fig. 6 *A*).

However, unlike activation, the inactivation process cannot be represented as a single-stage conformational transition related to movement of the gating charge, because the dependencies of α_{f2} and β_{f2} (kinetic scheme, Eq. 10) on potential have similar slopes (Fig. 6, *C* and *D*).

The membrane depolarization not only shifts the equilibrium toward channel inactivation but simultaneously increases the rate of forward and reverse steps of rapid inactivation. This is indirect evidence that the inactivation process involves additional rapid potential-dependent steps. Thus, an anomalous decrease in the rate of exit from rapid inactivation on depolarization, i.e., an increase in $\alpha_{f2}(E)$, suggests that for rapid inactivation, not scheme Eq. 10 but the following scheme is valid:

$$G_1' \underset{k_2}{\overset{k_1}{\leftrightarrow}} G_1 \underset{\beta_{f2}}{\overset{\alpha_{f2}}{\leftrightarrow}} G_0,$$

where G_1' is the state with closed inactivation gates, which cannot change to state G_O. Provided that k_1 and k_2 are much greater than α_{f2} and β_{f2}, i.e., states G'_1 and G_1 are related by the equilibrium relation $G_1' = k_1 \cdot G_1/k_2$, the equation for rapid inactivation of system Eq. 3 is then transformed to:

$$\dot{f}_2 = \frac{\alpha_{f2}}{1 + k_1/k_2}(1 - f_2) - \beta_{f2} f_2.$$

Hence, it follows that if the ratio k_1/k_2 sharply decreases on membrane depolarization, the effective rate constant of exit from inactivation $\alpha_{f2}/(1 + k_1/k_2)$ may increase.

There is another explanation for the unusual dependence of inactivation rate constants on potential, which is not related to the movement of inactivation gating charge. Studies of gating behavior of Na^+ (Gonoi and Hille, 1987; Cota and Armstrong, 1989), K^+ (Koren at al., 1990) and T-type Ca^{2+} channels (Chen and Hess, 1990) showed that transition of the channel to the inactivation state is virtually independent of membrane potential; i.e., the inactivation gating charge, if any, is very small. It may be assumed that in our case the dependence of inactivation on potential is a consequence of potential-dependent channel activation.

On the basis of the analysis of the effect of nifedipine on Ca^{2+} current, we propose a mechanism for Ca^{2+} channel inactivation (Fig. 7). This antagonist of L-type Ca^{2+} channels affects only the kinetics of activation and slow inactivation (Fig. 7, *top* and *middle*), leaving rapid inactivation unaltered (Fig. 7, *bottom*). The characteristic time of rapid inactivation τ_{f2} is insensitive to nifedipine. Thus, the effect of isoproterenol on activation and the anomalous dependence of α_{f2} and β_{f2} suggests that kinetics of rapid inactivation are mainly due to cAMP-dependent phosphorylation. It is unlikely that rapid inactivation is related to the activation process, because nifedipine-induced changes in activation kinetics should also have affected the kinetics of activation. It is also questionable that the inactivation proceeds by a current-dependent mechanism, given that Ca^{2+}

TABLE 3 Averaged steady-state characteristics of Ca^{2+} current inactivation

	Active animals	Hibernating animals	Hibernating animals + isoproterenol
$E_{f1}^{0.5}$, mV	−26.3 ± 3.9	−13.6 ± 4.9	−39.7 ± 3.9
k_{f1}, mV	−24.0 ± 2.6	−14.7 ± 1.1	−24.2 ± 2.1
$E_{f2}^{0.5}$, mV	23.1 ± 1.6	29.1 ± 2.9	16.4 ± 5.0
k_{f2}, mV	−24.6 ± 2.0	−15.7 ± 1.3	−22.5 ± 0.8

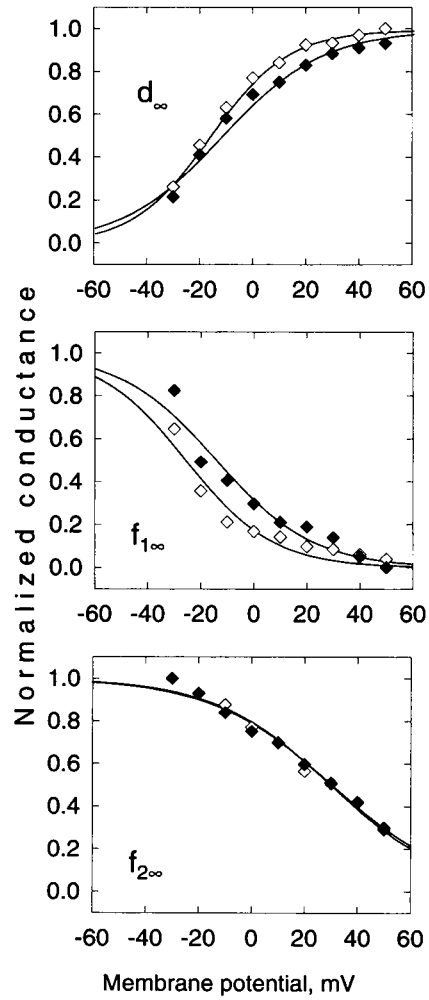

FIGURE 7 Normalized conductances calculated by fitting Ca^{2+} currents in nifedipine-treated cardiocyte using Eq. 5. ◇, without 5 μM nifedipine; ◆, with 5 μM nifedipine.

conductance, as determined by the slope of the right-hand branch of the current-voltage curve, was 2.87 nS in control and 0.99 nS in the presence of nifedipine. The peak current values also differ by threefold, and hence, the amount of Ca^{2+} entering across the channels decreases in proportion. However, as mentioned above, the normalized conductance of rapid inactivation remains unaffected. Presumably, the mechanism of current-dependent inactivation is realized in the case of slow inactivation, which will be discussed in the next section.

Kinetics of slow inactivation

The steady-state characteristics of slow inactivation kinetics and the results of Boltzmann approximation of normalized conductance are presented in Fig. 8 and Table 3. Slow inactivation is particular to late stages of Ca^{2+} currents, and characterized by long characteristic times and low rates of opening and closing of gates (α_{f1} and β_{f1} from kinetic scheme (Eq. 9)).

From Fig. 8 it can be seen that parameters of slow Ca^{2+} current inactivation in cardiocytes of active ground-squirrels, are shifted toward hyperpolarization by ~10 mV relative to those of hibernating animals. Addition of isoproterenol to cells of hibernating animals caused a significant (by ~20 mV) shift of the $E_d^{0.5}$ toward hyperpolarization.

The shape of the dependencies α_{f1} and β_{f1} on membrane potential varies with the state of animals (Fig. 8, *C* and *D*). In cardiocytes of active and hibernating animals in the presence of isoproterenol, both parameters decrease with increasing membrane potential; the curves have a similar slope, indicating that the process of slow inactivation cannot be represented as a simple single-stage conformational transition associated with movement of the gating charge. By contrast, in cardiocytes of hibernating animals, parameters α_{f1} and β_{f1} show opposite directed slopes.

Fig. 9 presents a typical experiment ($n = 4$) on the effect of isoproterenol on cardiocytes of hibernating animals. Isoproterenol increased the rate of the reverse transition β_{f1} approximately two- to threefold and changed the direction of the slope depending on membrane potentials. In terms of the conception of independence of activation and inactivation proposed in this study, this finding may be interpreted to indicate that slow inactivation represents both a potential- and current-dependent process. If the inward current is considerably (severalfold) reduced during hibernation or in response to nifedipine, the current-dependent inactivation does not affect the general inactivation process. In this case, only the first, the potential-dependent, inactivation component is retained. Interestingly, the inactivation gating charge calculated by fitting the data using Eq. 11 (Fig. 5 *A*) was much higher than it might be expected ($z_{f1} = -1.83 \pm 0.2$; $n = 3$ cardiocytes from hibernating animals). As in the case of activation, the effective gating charge is two times as great, since the model suggests the availability of two inactivation gates. An indirect confirmation of this interpretation is the fact that any agonist of the Ca^{2+} current shifts, as a rule, the steady state of slow inactivation toward hyperpolarization, because of initiation of a current-dependent process, whereas all antagonist (e.g., nifedipine, Fig. 7, *middle*) cause opposite directed changes in this parameter. Moreover, the rate constant of slow inactivation introduced

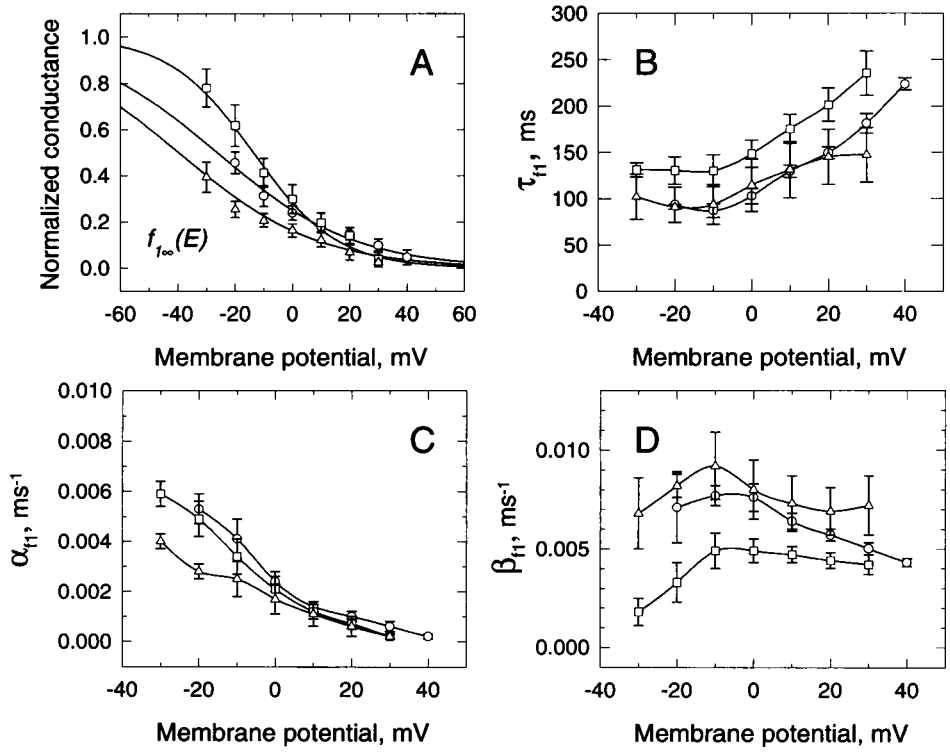

FIGURE 8 Averaged normalized conductance of slow Ca^{2+} current inactivation. *A*: Normalized conductance. Solid curves constructed using Eq. 5 (Table 3). *B*: Characteristic times. *C* and *D*: Rate constants of slow inactivation (kinetic scheme (Eq. 9)). (□) Hibernating; (○) active; (△) hibernating plus isoproterenol ($n = 5$).

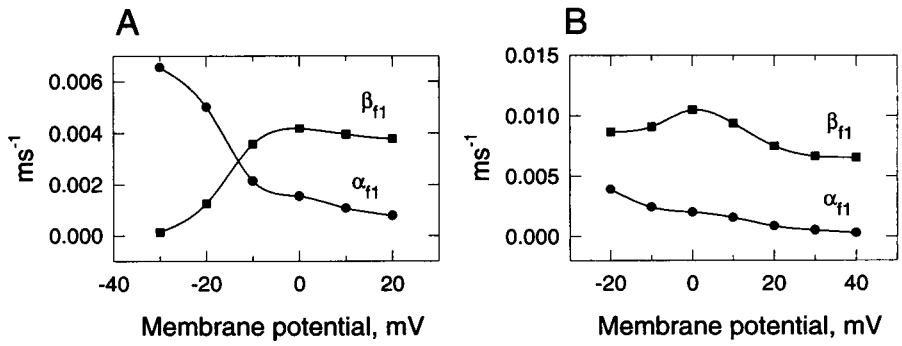

FIGURE 9 Rate constants of slow Ca^{2+} current inactivation (kinetic scheme (Eq. 9)) in cardiocytes of a hibernating ground squirrel in the absence (*A*) and presence of isoproterenol (*B*).

in the model of current-dependent inactivation (Standen and Stanfield, 1982; Markwardt and Nilius, 1988) is 0.005 ms^{-1}, which coincides almost completely with the slow inactivation rate constant in our model. To verify this hypothesis, experiments involving the determination of slow inactivation parameters at different extracellular Ca^{2+} concentrations are needed. Such experiments were not carried out in the framework of this study.

DISCUSSION

The present study investigated the properties of the L-type Ca^{2+} current in hibernators and developed a model that includes two activation gates, two f_1-type inactivation gates, and one f_2-type inactivation gate ($d^2f_1^2f_2$ model). The proposed kinetic model of the L-type calcium channel with its 18 stages appears rather extensive. This is primarily because of the principle of independence of the activation and inactivation processes on which this model is based. We could have, for instance, abandoned the principle of independence of the activation and inactivation processes, as was done by Chen and Hess (1990) in the description of the gating mechanism of the T-type calcium currents. This would have reduced the number of stages in the kinetic model, but would have made the mathematical description of Ca^{2+} current kinetics much more difficult and the interpretation of experimental data less obvious. It is for this reason that we considered dissecting the process of channel regulation into relatively independent stages.

The model used for analysis of the kinetic parameters appears to be adequate. In particular, the quadratic variable of activation, d^2, indicates the existence of two closed states, which correspond to the C1-C2–0 scheme of Ca^{2+} channel activation confirmed by experiments on single Ca^{2+} channels (Tsien et al., 1986). The effective valence of the charge related to the opening of one activation gate is equal to 1.5–2, which is in good agreement with measurements of gating currents related to the activation of cardiac L-type calcium channel (Neely et al., 1993; Bangalore et al., 1995). The entire activation process is associated with movement of the total gating charge (3–4) and is sensitive to a β-adrenoceptor agonist. Interesting, in our opinion, is a variation in the effective valence of activation gates from 1.5 (active ground squirrels) to 2 (hibernating animals). A possible reason for this variation is the loss of one or several negatively charged phosphate groups because of dephosphorylation, assuming that the phosphorylation site is in some way connected with the gate subunits (Tsien et al., 1988). It is also of interest that z_d of Ca^{2+} channels of hibernating ground squirrels returns to values close to 1.5 in response to isoproterenol (Table 2). Presumably, the modification of this conductance component is due only to a decrease in the number of phosphorylated channels induced by a reduction in catecholamine level during hibernation (Gainullin and Saxon, 1988; Florant et al., 1982).

The slow inactivation (f_1-type) is due to two processes, one of which is related to the gate mechanism and the other to the current-dependent inactivation. For hibernating animals, the total effective gating charge lies in the range between −3.5 and −4. In studies of Ca^{2+} channel kinetics, it is common to employ Ba^{2+}. It can be assumed that in our case, the function of rapid inactivation, f_2, in Eq. 3 is due to Ca^{2+}-induced inactivation of the Ca^{2+} channel. When we replaced Ca^{2+} by 2 mM Ba^{2+}, currents across Ca^{2+} channels showed a retarded inactivation. However, in this case we also failed to derive monotonic steady-state characteristics of conductance in the framework of Eq. 1, which suggests the existence of one inactivation component. Similarly, Markwardt and Nilius (1988) showed that although Ba^{2+} has a lower affinity for the calcium-binding site of the channels than Ca^{2+}, Ba^{2+} is involved in the inactivation of Ca^{2+} channels. It is by this mechanism the two-stage course of inactivation was explained. The rate constants for rapid and slow inactivation used in their calculations were 0.8 ms^{-1} and 0.005 ms^{-1}, respectively. The rate constants derived with our model are consistent with these values (Figs. 6, 8, 9). Hadley and Lederer (1991) showed that Ca-dependent inactivation is sensitive to β-adrenergic stimulation. In terms of the proposed model, we were able to separate the inactivation component. This conductance component was found to be completely insensitive even to a threefold decrease in inward Ca^{2+} current induced by nifedipine.

Differences in the current kinetics between active and hibernating animals were observed for all components. In hibernating ground squirrels, the most pronounced shift toward depolarizing potentials was observed for the steady-

state conductance of both inactivation components, whereas on activation the shift was smaller. The characteristic times (τ_d, τ_{f1}, τ_{f2}) for all three components of Ca^{2+} current conductance in hibernating ground squirrels were found to be 1.5 times smaller than in active animals.

Isoproterenol reversed the characteristic times to values close to those of active animals, shifting simultaneously the normalized conductance toward polarizing potentials by values exceeding the difference in conductance between active and hibernating ground squirrels. This observation appears to be paradoxical to some extent, because the restoration of the kinetic parameters induced by phosphorylation of channels in hibernating animals does not govern the increase in Ca^{2+} current amplitude to values recorded in active animals in response to isoproterenol (Alekseev et al., 1994). Therefore, the change in the amplitude of Ca^{2+} current during hibernation may be due to a seasonal decrease in the single channel conductance and/or in the number of Ca^{2+} channels activated on depolarization during hibernation. Another possibility of suppression of the Ca^{2+} current may be related to the cGMP-dependent channel phosphorylation (Wahler et al., 1990; Tohse and Sperelakis, 1991). However, the role of the cGMP-dependent protein kinase in hibernating cycles requires additional investigation. Thus, the question related to mechanisms responsible for the decrease in the number of Ca^{2+} channels and/or the maintenance of these channels in a non-active state remains open.

The study was supported by grants from the Russian Foundation of Fundamental Investigations (nos. 93–04-21784 and 95–04-12193a) and International Science Foundation (nos. RN1000 and RN1300), the American Heart Association, and the National Heart Foundation, a program of the American Health Assistance Foundation.

REFERENCES

Adams, D. J., and P. W. Gage. 1979. Ionic currents in response to membrane depolarization in an *Aplysia* neuron. *J. Physiol.* 389:115–141.

Alekseev, A. E., A. F. Korystova, D. A. Mavlyutova, and Y. M. Kokoz. 1994. Potential-dependent Ca currents in isolated heart cells of hibernators. *Biochem. Mol. Biol. Int.* 33:365–376.

Bangalore, R., M. Mehrke, K. Gingrich, F. Hofmann, and R. S. Kass. 1995. Gating currents of recombinant cardiac L-type calcium channels expressed in human embryonic kidney (HEK-293) cells: relationship between charge movement and ionic current. *Biophys. J.* 68:A14.

Burlington, R. F., M. S. Dean, and S. B. Jones. 1989. Coronary autoregulation and metabolism in hypothermic rat and ground squirrel hearts. *Am. J. Physiol.* 256 (2 Pt 2):R357–365.

Chen, C., and P. Hess. 1990. Mechanism of gating of T-type calcium channels. *J. Gen. Physiol.* 96:603–630.

Cota, G., and C. M. Armstrong. 1989. Sodium channel gating in clonal pituitary cells: the in-activation step is not voltage dependent. *J. Gen. Physiol.* 94:213–232.

Duker, G. D., S.-O. Olsson, N. H. Hetch, J. B. Senturia, and B. W. Johansson. 1983. Ventricular fibrillation in hibernators and nonhibernators. *Cryobiology.* 20:407–420.

Duker, G. D., P.-O. Sjoquist, O. Svensson, B. Wohlfart, and B. W. Johansson. 1986. Hypothermic effect on cardiac action potentials: difference between a hibernator, hedgehog, and a nonhibernator, guinea pig. *In* Living in the Cold: Physiological and Biochemical Adaptations. H. C. Heller, X. J. Musacchia, and L. C. H. Wang, editors. Elsevier, New York. 565- 571.

Fabiato, A., and C. M. Baumgarten. 1984. Methods for detecting calcium release from the sarcoplasmic reticulum of skinned cardiac cells and the relationship between calculated transsarcolemmal calcium movements and calcium release. *In* Function of the Heart in Normal and Pathological States. N. Sperelakis, editor. Martinus Nijhoff, Boston. 215–254.

Fabiato, A., and F. Fabiato. 1979. Calcium and cardiac excitation-contraction coupling. *Annu. Rev. Physiol.* 41:473–484.

Florant, G. U., E. D. Weitzman, A. Jayant, and L. J. Cote. 1982. Plasma catecholamine level during cold adaptation and hibernation in woodchucks (*Mormota menax*). *J. Therm. Biol.* 7:143–146.

Gainullin, R. Z., and M. E. Saxon. 1988. Mechanism of depression of calcium electrogenesis in the ventricular muscle during hibernation. *Cryo Lett.* 9:392–403.

Gonoi, T., and B. Hille. 1987. Gating of Na channels. Inactivation modifiers discriminate among models. *J. Gen. Physiol.* 89:253–274.

Hadley, R. W., and W. J. Lederer. 1991. Ca^{2+} and voltage inactivate Ca^{2+} channels in guinea-pig ventricular myocytes through independent mechanisms. *J. Physiol.* 444:257–268.

Hagiwara, S., and S. Nakajima. 1966. Differences in Na and Ca spikes as examined by application of tetrodotoxin, procaine and manganese ions. *J. Gen. Physiol.* 49:793–806.

Heldmaier, G., and T. Ruf. 1992. Body temperature and metabolic rate during natural hypothermia in endotherms. *J. Comp. Physiol. B. Biochem. Syst. Environ. Physiol.* 162:696–706.

Herve, J. C., K. Yamaoka, V. W. Twist, T. Powell, J. C. Ellory, and L. C. H. Wang. 1992. Temperature dependence of electrophysiological properties of guinea pig and ground squirrel m /ocytes. *Am. J. Physiol.* 263:R177–R184.

Himmelblau, D. M. 1972. Applied nonlinear programming. McGraw-Hill Book Co., Austin, Texas.

Hodgkin, A. L., and A. F. Huxley. 1952. Current carried by sodium and potassium ions through the membrane of the giant axon of *Loligo. J. Physiol.* 116:449–472.

Imaizumi, Y., K. Muraki, M. Takeda, and M. Watanabe. 1989. Measurement and simulation of noninactivating Ca current in smooth muscle cells. *Am. J. Physiol.* 256:C880–C885.

Kondo, N. 1986a. Excitation-contraction coupling in hibernating chipmunk myocardium. *Experientia.* 42:1220–1222.

Kondo, N. 1986b. Excitation-contraction coupling in myocardium of nonhibernating and hibernating chipmunks: effect of isoprenaline, a high calcium medium and ryanodine. *Circ. Res.* 59:221–228.

Kondo, N. 1987. Identification of prehibernating state in myocardium from hibernating chipmunks. *Experientia.* 43:873–875.

Kondo, N., and J. Kondo. 1993. Identification and characterization of novel types of plasma protein specific for hibernation in rodents. *In* Life in the Cold. C. Carey, G. L. Florant, B. A. Wunder, and B. Horowitz, editors. Westview Press, Boulder, CO. 469–473.

Kondo, N., and S. Shibata. 1984. Calcium source for excitation-contraction coupling in myocardium of non-hibernating and hibernating chipmunks. *Science.* 225:641–643.

Koren, G., E. R. Liman, D. E. Logothetis, B. Nadal-Ginard, and P. Hess. 1990. Gating mechanism of a cloned K-channel expressed in frog oocytes and mammalian cells. *Neuron.* 4:39–51.

Korn, S. J., A. Marty, J. A. Connor, and A. Horn. 1991. Perforated patch recording. *Methods Neurosci.* 4:264–373.

Kurachi, Y., Y. Asano, R. Tarkikawa, and T. Sigumoto. 1989. Cardiac Ca current does not run down and is very sensitive to isoprenaline in the nystatine-method of whole cell recording. *Naunyn-Schmiedebergs. Arch. Pharmakol.* 340:219–222.

Langton, P. D., E. P. Burke, and K. M. Sanders. 1989. Participation of Ca currents in colonic electrical activity. *Am. J. Physiol.* 257:C451–C460.

Liu, B., L. C. H. Wang, and D. D. Belke. 1991. Effect of low temperature on the cytosolic free Ca in rat ventricular myocytes. *Cell Calcium.* 12:11–18.

Lyman, C. P., J. S. Willis, A. Malan, and L. C. H. Wang. 1982. Hibernation and Torpor in Mammals and Birds. Academic Press, New York.

Markwardt, F., and B. Nilius. 1988. Modulation of calcium channel currents in guinea-pig single ventricular heart cells by the dihydropyridine BAY K 8644. *J. Physiol.* 399:559–575.

Neely, A., X. Wei, R. Olcese, L. Birnbaumer, and E. Stefani. 1993. Potentiation by the β subunit of the ratio of the ionic current to the charge movement in the cardiac calcium channel. *Science.* 262: 575–577.

Saxon, M., and R. Gainullin. 1989. Differential effect of the dihydropyridine calcium channel activator, CGP28392 and the cyclic AMP system activator, noradrenaline on the negative force staircase in ventricular myocardium from the hibernating ground squirrels. *Cryo Lett.* 10:51–58.

Schneider, M. F., and W. K. Chandler. 1973. Voltage dependent charge movement in skeletal muscle: a possible step in excitation-contraction coupling. *Nature.* 242:244–246.

Smith, T. W., K. Yamaoka, V. W. Twist, J. C. Ellory, T. Powell, and L. C. H. Wang. 1989. Membrane transport in isolated cardiac myocytes of ground squirrels: cold sensitivity of pump and channels. *In* Living in the Cold II. A. Malan and B. Canguilhem, editors. Colloque INSERM/John Libbey Eurotext Ltd., London. 177–184.

Snapp, B. D., and H. C. Heller. 1981. Suppression of metabolism during hibernation in ground squirrels (*Citellus lateralis*). *J. Physiol. Zool.* 54:297–307.

Standen, N. B., and P. R. Stanfield. 1982. A binding-site model for calcium channel inactivation that depends on calcium entry. *Proc. R. Soc. Lond. Biol. Sci.* 217:101–110.

Tohse, N., and N. Sperelakis. 1991. cGMP inhibits the activity of single calcium channels in embryonic chick heart cells. *Circ. Res.* 69:325–331.

Tsien, R. W., B. P. Bean, P. Hess, J. B. Lansman, B. Nilius, and M. C. Nowycky. 1986. Mechanisms of calcium channel modulation by β-adrenergic agents and dihydropyridine calcium agonists. *J. Mol. Cell Cardiol.* 18:691–710.

Tsien, R. W., A. P. Fox, L. D. Hirning, D. Lipscombe, D. V. Madison, E. W. McCleskey, R. J. Miller, M. Poenie, H. Reuter, S. A. Thayer, and R. Y. Tsien. 1988. Calcium channels, calcium stores and norepinephrine release in sympathetic neurons. *In* Molecular Mechanisms in Secretion. N. A. Thorn, M. Treiman, and O. H. Petersen, editors. Munksgaard, Copenhagen. 66–84.

Wahler, G. M., N. Rusch, N. Sperelakis. 1990. 8-bromo-cyclic GMP inhibits the calcium channel current in embryonic chick ventricular myocytes. *Can. J. Physiol. Pharm.* 68:531–534.

Wang, L. C. H. 1978. Energetics and field aspects of mammalian torpor: the Richardson's ground squirrel. *In* Strategies in cold: Natural Torpidity and Thermogenesis. L. C. H. Wang and J. W. Hudson, editors. Academic Press, London. 109–145.